Author(s): Savin, Hele & Kuivalainen, P. & Novikov, S. & Lebedeva, N.

Title: Magnetic polaron formation in graphene-based single-electron transistor

Year: 2014

Version: Post print

Please cite the original version:

Savin, Hele & Kuivalainen, P. & Novikov, S. & Lebedeva, N. 2014. Magnetic polaron formation in graphene-based single-electron transistor. Physica Status Solidi B. Volume 251, Issue 4. 1-15. DOI: 10.1002/pssb.201350295.

Magnetic polaron formation in a ferromagnetic graphene-based single-electron transistor

H. Savin, P. Kuivalainen*, S. Novikov, and N. Lebedeva

Department of Micro and Nanosciences, School of Electrical Engineering, Aalto University, P.O. Box 13500, FI-00076 Aalto, Espoo, Finland

*Corresponding author: e-mail pekka.kuivalainen@aalto.fi, Phone +358 50 307 5117, Fax +358 9 470 25008

Keywords magnetic insulators, spintronics, ferromagnetism, graphene

We theoretically study the magnetic polaron (MP) formation in a ferromagnetic graphene single-electron transistor (SET), which consists of a graphene quantum dot (QD) between two insulating layers, i.e., a ferromagnetic insulator EuO and a nonmagnetic substrate such as SiC. In the lateral direction the QD is electrically coupled to source, drain and gate electrodes, so that the number of electrons can be controlled by the gate voltage. Due to a proximity effect at the EuO/graphene interface, i.e., the exchange interaction between the charge carriers in graphene and the localized magnetic electrons in EuO, there is a magnetic coupling between the graphene QD and EuO. Using Green's function technique an expression for the total free energy of the SET is derived, which then is minimized at the given temperature and gate voltage. This leads to the MP formation and a consequent local enhancement of the ferromagnetic properties of EuO at the EuO/graphene interface. The MP formation is enforced by the large Coulomb interaction between the carriers in graphene. The spin polarization at the graphene/EuO interface in the QD area can be controlled by the gate voltage of the SET.

1 Introduction Graphene has attracted enormous interest because of its unusual physical properties and also because of its potential applications in carbon based electronics [1-5]. Due to small spin-orbit coupling and long spin lifetimes graphene also is a promising material for spintronic applications (see ref. [6] and refs therein). Several approaches to control the spin-dependent phenomena in graphene nanostructures have been proposed. Graphene quantum dots (QDs) have been identified as an ideal host for spin qubits [7, 8]. Recently the first graphene QDs and single-electron transistors were fabricated with features as small as 10 nm [9-11]. Also spin polarized states induced by the edge defects in zigzag graphene nanoribbons have been studied [12-15]. Spin injection from ferromagnetic Co into graphene has been achieved [16], and recently highly efficient spin transport in epitaxial graphene on SiC has been reported showing spin transport efficiencies up to 75% and spin diffusion lengths exceeding 100 μm [17]. Also it has been predicted theoretically that graphene nanomesh structure should show magnetic properties [18].

An alternative approach to graphene spintronics has been proposed by considering ferromagnetic insulator (FMI)-on-graphene structures [19, 20]. In these devices the spin manipulation is achieved

via the exchange interaction between the charge carriers in graphene and the localized magnetic electrons of the magnetic atoms in the FMI. Also the possibility to control the spin dependent electrical current using a ferromagnetic gate has been discussed in several works [21-25]. Due to the spin splitting of the electronic states a spin polarized current is generated, and it can be controlled by the gate voltage. A drawback in these structures is that due to the lack of the energy band gap, the spin polarization in a 2D monolayer graphene is limited [21-23]. The situation is more favorable in bilayer graphene due to its specific electronic structure, as discussed by Semenov et al. [25] and Hung Nguyen et al. [26]. Strong resonant tunneling effects and large magnetoresistance behavior have been predicted [26, 27] in the case of the ferromagnetic insulator/bilayer graphene-structures. The value of the strength of the exchange interaction at the graphene/FMI interface is unknown so far, but in the case of the EuO/Al-system an experimental estimate J_{exch}=15 meV for the exchange coupling parameter has been reported [28]. This value would be large enough to cause, e.g., a significant spin splitting of the electronic states in graphene [23]. Recently even a much larger value for the exchange parameter in an EuO/graphene-system was estimated based on first-principle calculations [29].

In the present paper we theoretically study the properties of a ferromagnetic graphene SET, which consists of a FMI layer on top of a graphene QD connected to drain, source and gate electrodes, also made of graphene. Especially we study the magnetic polaron (MP) formation inside the QD in the case where the graphene/FMI structure is on a SiC substrate, which transforms the relativistic massless Dirac fermions in graphene into ordinary charge carriers having a mass. The EuO/graphene/SiC-structure was chosen as a model system, because EuO is an ideal isotropic ferromagnetic insulator, the magnetic properties of which are well known. Furthermore, the fabrication of ferromagnetic EuO thin films on graphene has been demonstrated recently [30, 31]. The advantage of the SiC substrate is that an existence of a band gap has been reported in the graphene/SiC system [32]. Later the results of Zsou et al. [32] have been questioned by other groups [33-35]. However, there are alternative proposals for insulating substrates or nanostructures, which also should induce a band gap in graphene, such as hexagonal boron nitride (h-BN) [36], graphene nanomesh [37], hydrogenated h-BN [38], and nanoperforated graphene [39]. Therefore, our assumption of a band gap in graphene is reasonable. The magnetic polaron means a coupled system consisting of a charge carrier together with the enhanced spin polarization of the magnetic lattice around the carrier. The MP formation has been studied intensively, both theoretically [40-47] and experimentally [48-53] in the case of anti- or paramagnetic II-VI compound semiconductors. Recently we have extended the theoretical treatment to ferromagnetic III-V compound semiconductor QDs and SETs [54, 55]. In the present paper we properly modify our previous model and apply it to graphene/FMI QDs and SETs. An important difference between the QDs made of ordinary magnetic semiconductors and those made of graphene is the smaller permittivity in graphene. This results in, e.g., a much larger Coulombic interaction between the confined charge carriers inside the graphene QD.

2 Model We study the ferromagnetic graphene SET structure shown in Fig.1. The epitaxial single layer graphene is sandwiched between an insulating substrate and a ferromagnetic insulator (FMI). The graphene QD is separated from the source (S) and the drain (D) electrodes by thin potential barriers. The electrical coupling between the electrodes and the QD is due to the tunneling of the carriers through the thin barriers. A simplified energy diagram vs. position is shown in Fig.1 (c). The value of the Fermi energy E_F can be controlled by the gate voltage V_g. We assume that E_F is a linear function of V_g, and that at zero bias the bottom of the dot potential is equal to E_F, as shown in Fig.1 (c). In the treatment of the MP formation we only consider the electrons that take part in electrical conduction in the Coulomb blockade (CB) regime. Then we only take into account the two uppermost singly occupied energy levels with energies ε_d^0 and $\varepsilon_d^0 + U$, as shown in Fig.1 (c). Here U is the Coulomb repulsion parameter between two electrons inside the graphene QD. The lower energy levels below ε_d^0 are assumed to be irrelevant for the charge transport and the MP formation. The number of electrons in the graphene QD can be controlled by the gate voltage. In the case of the simple model system shown in Fig.1 the QD occupancy can be 0, 1, or 2, depending on the occupancy of the levels ε_d^0 and $\varepsilon_d^0 + U$.

In our model system a SiC substrate was chosen, because it generates a band gap in the electronic structure of graphene, which changes the massless Dirac fermions into ordinary charge carriers with a finite mass. Zhou et al. [32] have shown that in an epitaxial graphene on the SiC substrate the band gap E_g = 0.26 eV is induced, when the graphene-sublattice interaction breaks the sublattice symmetry. Independent of the origin of the band gap the energy bands in the graphene/SiC system near the band edge are given by

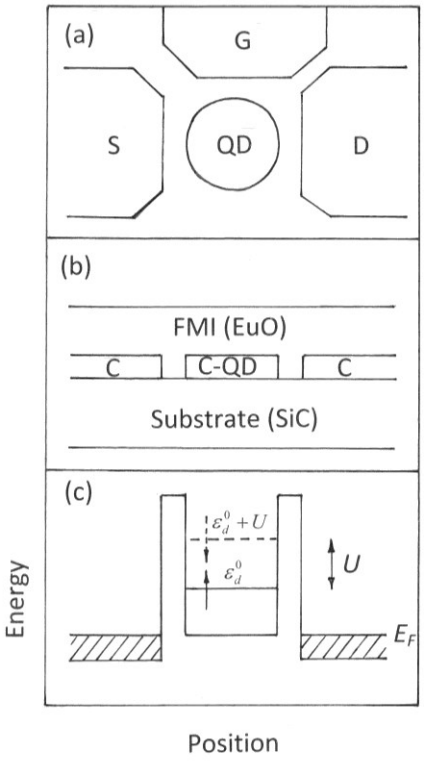

Fig.1. (a) Top view of the graphene SET including the graphene quantum dot (QD) and source (S), drain (D) and gate (G) electrodes. (b) Cross section of the graphene SET including the ferromagnetic insulator layer (FMI) on top of the graphene quantum dot (C-QD) and the graphene electrodes (C), all on a SiC substrate. (c) Energy diagram vs. position for a ferromagnetic SET showing the potential barriers that separate the QD from the source and drain electrodes. ε_d^0 and $\varepsilon_d^0 + U$ are the two spin degenerate dot energy levels that participate the charge transport through the SET. The Zeeman splitting of these energy levels is not shown. *U* is the Coulomb repulsion energy between two electrons in the QD. The bottom of the dot potential is assumed to be equal to the Fermi energy E_F, when the gate voltage of the SET is zero.

$$E(\mathbf{k}) = \pm\sqrt{\left(\frac{E_g}{2}\right)^2 + \hbar \quad ^2} \tag{1}$$

where v_F is the Fermi velocity and $\mathbf{k}$ is the carrier wave vector. The plus (minus) sign refers to the conduction (valence) band. At low excitation energies close to the minimum in the conduction band we can calculate the effective mass as in ordinary semiconductors:

$$m^* = \hbar^2 \left(\frac{\partial^2 E(\mathbf{k})}{\partial \mathbf{k}^2}\right)^{-1} = \frac{E_g}{2v_F^2} \tag{2}$$

Now we can treat the electrons inside the disc-like graphene QD with a radius R_0 as ordinary charge carriers, as we did in our previous paper in the case of magnetic semiconductor QDs [54, 55].

In the CB regime a SET can be described by the Anderson Hamiltonian [56, 57], which is given by

$$H_A = \sum_{\substack{\mathbf{k}\in S,D \\ \sigma}} E(\mathbf{k}\sigma) c^{\dagger}_{\mathbf{k}\sigma} c_{\mathbf{k}\sigma} + \sum_{\sigma} \varepsilon^0_{d\sigma} d^{\dagger}_{\sigma} d_{\sigma} + U n_{\uparrow} n_{\downarrow} + \sum_{\substack{\mathbf{k}\in S,D \\ \sigma}} \left(V_{\mathbf{k}\sigma} c^{\dagger}_{\mathbf{k}\sigma} d_{\sigma} + h.c. \right) \tag{3}$$

Here $c^{\dagger}_{\mathbf{k}\sigma}$ ($c_{\mathbf{k}\sigma}$) creates (destroys) a spin-σ charge carrier with momentum $\hbar$ and energy $E(\mathbf{k}\sigma)$ given by (1) in the source (S) or drain (D) regions. $d^{\dagger}_{\sigma}$ (d_{σ}) creates (destroys) an electron with spin σ at the non-interacting energy level $\varepsilon^0_{d\sigma}$ in the QD region, and $n_{\sigma} = d^{\dagger}_{\sigma} d_{\sigma}$ with $\sigma = \uparrow$ or $\downarrow$ is the occupation number operator. The last term in the Hamiltonian (3) is the hybridization of the dot region to the source and drain electrodes via tunneling, which gives rise to a lead coupling $\Gamma_{\sigma} = \Gamma^S_{\sigma} + \Gamma^D_{\sigma}$ with $\Gamma^{S(D)}_{\sigma} = 2\pi \sum_{\mathbf{k}\in S(D)} |V_{\mathbf{k}\sigma}|^2 \, \delta\left(E - E(\mathbf{k}\sigma)\right)$. The Hamiltonian (3) gives an adequate description for the relevant electronic structure of the dot in a nonmagnetic SET. However, in the case of the ferromagnetic SET we must add to (3) the Heisenberg Hamiltonian H_{m} describing the ferromagnetic subsystem (FMI in Fig.1) and also the exchange interaction H_{exch} between the charge carrier spin in graphene and the localized magnetic moments of the magnetic atoms at the graphene/FMI interface. The former is given by

$$H_m = -\sum_{\mathbf{R},\mathbf{R}'} I(\mathbf{R},\mathbf{R}') \mathbf{S}_{\mathbf{R}} \cdot \mathbf{S}_{\mathbf{R}'} - g_L \mu_B B \sum_{\mathbf{R}} S^z_{\mathbf{R}} \tag{4}$$

where $I(\mathbf{R},\mathbf{R}')$ is the ferromagnetic coupling constant between the magnetic atoms, and $\mathbf{S}_{\mathbf{R}}$ is the spin operator for the total spin of the magnetic atom at a lattice site $\mathbf{R}$. The last term in (4) gives the ordinary Zeeman energy when an external magnetic field $\mathbf{B}$ is in the z-direction. Using the Hamiltonian (4) the average spin polarization $\langle S^z_{\mathbf{R}} \rangle$ of the magnetic atoms can be calculated in the mean-field approximation. The exchange interaction H_{exch} is given by

$$H_{exch} = -\sum_{\mathbf{R}} J_{exch}(\mathbf{r}-\mathbf{R}) \frac{\boldsymbol{\sigma}}{2} \cdot \mathbf{S}_{\mathbf{R}} \tag{5}$$

where $J_{exch}(\mathbf{r}-\mathbf{R})$ is the exchange interaction potential, which is assumed to be of the contact-type, $J_{exch}(\mathbf{r}-\mathbf{R}) \propto J_{exch}\delta(\mathbf{r}-\mathbf{R})$, and J_{exch} is the exchange interaction parameter (constant). The interaction (5) leads to the spin-polarized energy levels in the QD region due to the giant Zeeman effect :

$$\varepsilon^{(1)}_{d\sigma} = \varepsilon^0_{d\sigma} - \frac{\Delta}{2}\left(\delta_{\sigma\uparrow} - \delta_{\sigma\downarrow}\right) \tag{6}$$

with

$$\Delta = J_{exch} \Omega_U \sum_{\mathbf{R}} |\psi_0(\mathbf{R})|^2 \langle S^z_{\mathbf{R}} \rangle \tag{7}$$

Here $\Omega_U = S_{area}/N$, S_{area} is the area of the device, and the summation over $\mathbf{R}$ goes through the magnetic atoms at the graphene/FMI interface, the number of which is *N*. In the variational calculation of the minimum in the total energy for the ferromagnetic QD we use as a two dimensional trial wave function the ground state wave function $\psi_0(\rho) \propto \exp\left(-\rho^2/l_\omega^2\right)$ for a cylindrical QD [58]. Here $\rho = (x, y)$ and l_ω is the decay parameter, which we shall use as a variational parameter when seeking the minimum of the total energy. Then the unperturbed dot energy ε_d^0 in (6) is given by

$$\varepsilon_{d\sigma}^0 = \frac{\hbar^2}{2m^* l_\omega^2} + \frac{1}{2} m^* \omega^2 l_\omega^2 \tag{8}$$

where ω is the confining parameter of the QD.

The retarded Green's function for the total Hamiltonian $H_{tot} = H_A + H_m + H_{exch}$ can be calculated in the same way as in the case of nonmagnetic quantum dots [59, 60] using the equation-of-motion technique. The final result is given by

$$G_\sigma(E) = \frac{1 - \langle n_{\bar{\sigma}} \rangle}{E - \varepsilon_{d\sigma}^{(1)} - \Sigma_\sigma(E)} + \frac{\langle n_{\bar{\sigma}} \rangle}{E - \varepsilon_{d\sigma}^{(1)} - U - \Sigma_\sigma(E)} \tag{9}$$

where $\bar{\sigma}$ denotes the opposite spin to σ. The average occupation numbers can be calculated using Green's function (9) and the fluctuation-dissipation theory [60]:

$$\langle n_\sigma \rangle = -\int d\omega n_F(\omega) \operatorname{Im} G_\sigma(\omega + i\varepsilon)/\pi \tag{10}$$

Here $n_F(\omega)$ is the Fermi-Dirac distribution function. The equations (9) and (10) are interrelated, which means that they must be solved self-consistently. In the case of the magnetic SET the self-energy $\Sigma_\sigma(E) = \Sigma_T^\sigma(E) + \Sigma_{exch}^\sigma(E)$ in Green's function (9) includes the tunnelling contribution Σ_T^σ as well as a contribution Σ_{exch}^σ from the exchange interaction (5).

The total free energy of the QD can be divided into two parts as

$$F_{tot} = F_c + F_m \tag{11}$$

where F_c is the contribution from the electronic subsystem, and it can be expressed as

$$F_c = -\sum_\sigma \int \frac{dE}{2\pi} n_F(E) \left[2 \operatorname{Im} G_\sigma(E) \right] E \tag{12}$$

The second term in (11) is the contribution from the magnetic subsystem. Following the previous treatments of the magnetic polarons in QDs [42, 43], we employ the local mean-field theory (LMFT) in the calculation of the magnetic properties of the ferromagnetic graphene QD. The

effective molecular field $B_{eff}(\mathbf{R})$ acting on the magnetic atoms and including the spins of the charge carriers can be derived by calculating the poles of the Green's function $<< S^{+}_{\mathbf{R}}, S^{-}_{\mathbf{R}'} >>$ [61]:

$$B_{eff}(\mathbf{R}) = B + 2\sum_{\mathbf{R}'} I(\mathbf{R},\mathbf{R}')\langle S^{z}_{\mathbf{R}'}\rangle / g_L\mu_B + \frac{J_{exch}\Omega}{2}\left(\langle n_{\uparrow}\rangle - \langle n_{\downarrow}\rangle\right)|\psi_0(\mathbf{R})|^2 / g_L\mu_B \quad (13)$$

The first two terms in (13) describe the ordinary molecular field acting on the magnetic atoms in a ferromagnetic system, whereas the last term gives the molecular field due to the charge carrier spin polarization $\langle n_{\uparrow}\rangle - \langle n_{\downarrow}\rangle$. This is the molecular field that causes the MP effect.

The average spin polarization of the magnetic atoms is calculated in the large dot limit, i.e., assuming that the number of magnetic atoms in contact with the dot is so large that the magnetic properties of the dot/FMI interface are similar to those of the bulk ferromagnet. Then, using LMFT the average spin polarization is a continuous function of position, and it is given by

$$\langle S^{z}_{\mathbf{R}}\rangle = SB_S\left(g_L\mu_B B_{eff}(\mathbf{R}) / k_B T\right) \quad (14)$$

where B_S is the Brillouin function for a magnetic atom with the total spin quantum number S. The magnetic part of the free energy F_m can be calculated in the usual way [42, 43, 54, 55], and the MP binding energy is defined as the energy difference

$$\Delta F_{tot} = F_{tot}\left(\langle S^{-}_{\vec{R}/\!/}\rangle\right) - F_{tot}\left(\langle S^{z}\rangle\right) \quad (15)$$

where $F_{tot}\left(\langle S^{-}_{\vec{R}/\!/}\rangle\right)$ is calculated in the case of the inhomogeneous position dependent spin polarization $\langle S^{-}_{\vec{R}/\!/}\rangle$ induced by the effective molecular field (13), whereas $F_{tot}\left(\langle S^{z}\rangle\right)$ is calculated in the case $|\psi_0| = 0$ in (13), i.e., by neglecting the effect of the charge carrier spins on the average spin polarization at the graphene/EuO interface. This allows us to calculate the total free energy as a function of the wave function decay parameter l_{ω}, which is used as a variational parameter. The MP is considered stable, if $\Delta F_{tot} < 0$.

3 Results and discussion We have calculated the local spin polarization at the graphene QD/FMI interface and the MP binding energy in the case where the FMI layer in the SET structure shown in Fig.1 is a ferromagnetic EuO thin film. We have chosen EuO as the FMI layer since it is an almost ideal ferromagnet, the magnetic properties of which can be described accurately using the Brillouin function (see Eq. (16)). Furthermore, EuO can be fabricated in a straightforward manner by oxidizing at low temperatures a metallic Eu thin evaporated on top of the single layer graphene. The radius of the two-dimensional disc-like graphene QD is R_0=10 nm. The other parameters used in the calculation are the following: Curie temperature T_C=70 K (EuO), lattice constant a_0=5.14 (EuO), Fermi velocity v_F=10^6 m/s (graphene), band gap E_g=0.26 eV (graphene on SiC), and the spin

quantum number *S*=7/2 (Eu atoms). The charging energy $U = \langle \psi_0 | e^2 / 4\pi\varepsilon_s r | \psi_0 \rangle$, which in ordinary semiconductor QDs with features 20 nm and permittivity $\varepsilon_S \approx 10$, is a few meVs, is much larger in graphene QDs due to the much smaller permittivity [40]. Since the exact value of *U* is unknown, we have performed the calculations using two different values, *U*=0.02 eV and *U*=0.1 eV. In the wide band width limit the total level broadening parameter $\Gamma = \mathrm{Im}\{\Sigma\}$ is assumed to be constant with the value 4 meV. The numerical tests showed that the MP formation depends very weakly on the level broadening. The most important material parameter in the ferromagnetic graphene SET is the exchange interaction coupling J_{exch} . Unfortunately, so far no experimental data for this parameter are available in the case of the graphene/EuO interface. However, based on the experimental results obtained in a EuO/Al system, a value J_{exch}=15 meV has been estimated previously [18]. Recently even a much higher value for J_{exch} was estimated based on first principle calculations [29]. Also in the case of other FMIs higher values, such as J_{exch}=0.065 eV, have been suggested [16]. However, all the estimated values are still much smaller than the experimental value J_{exch}=0.17 eV for bulk EuO [41]. Due to the lack of experimental results for the exact strength of the exchange interaction in the graphene/EuO structure we have calculated the properties of the MP in the cases of weak (J_{exch}=0.02 eV) and intermediate (J_{exch}=0.05 eV) couplings.

Fig.2 shows the average spin polarization at the graphene/EuO interface at the centre of the graphene QD (*R*=0) and the MP binding energy vs. temperature, when the gate voltage is 0.8 V. The original Curie temperature of EuO, T_C=70 K, increases to 92 K in the case of the intermediate coupling (J_{exch}=0.05 eV). Also in the case of the weak coupling (J_{exch}=0.02 eV) the MP formation occurs (Fig.2 (b)), especially at temperatures close to T_C, but now the increase in T_C is only about 3 K. The results show that there is a significant increase in the local spin polarization and the clear MP formation even in the case of the weak coupling.

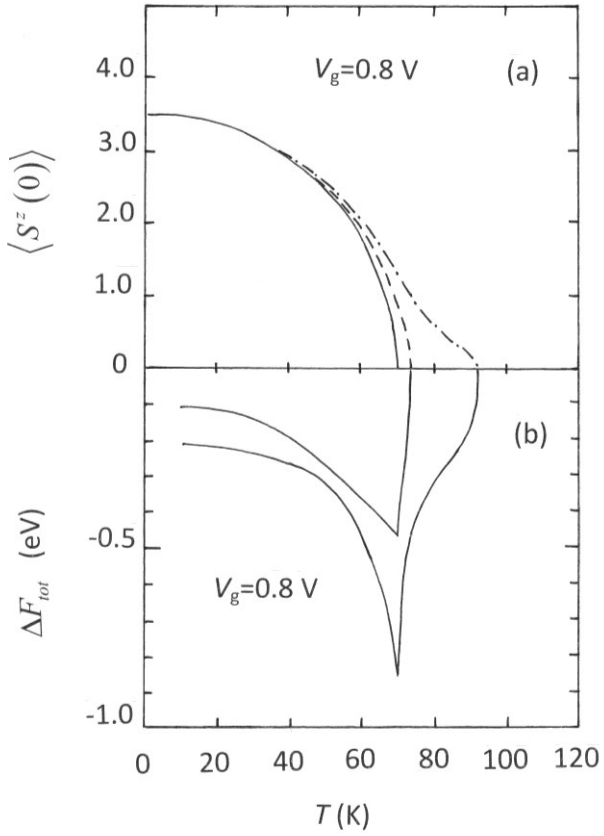

Fig.2. (a) Average spin polarization of the magnetic Eu atoms at the graphene/EuO interface at the centre of the QD (R=0) as a function of temperature at the gate voltage 0.8 V and in the case U=0.1 eV. The solid curve shows the original spin polarization vs. temperature in EuO, when the MP formation is neglected. The dashed curve has been calculated in the case of a weak coupling, J_{exch}=0.02 eV, and the dash-dotted curve in the case of the intermediate coupling, Jexch=0.05 eV, the MP formation included in both cases. (b) MP binding energy vs. temperature in the cases J_{exch}=0.02 eV (the upper curve) and J_{exch}=0.05 eV (the lower curve), when the gate voltage is 0.8 V.

Figs. 3 and 4 show the gate voltage dependence of the average spin polarization at the graphene/EuO interface at the centre of the QD (R=0). The results of Fig.3 have been calculated in the case of the intermediate coupling (J_{exch}=0.05 eV), and those in Fig.4 in the case of the weak coupling (J_{exch}=0.02 eV), both at T=T_C=70 K. An interesting result is that a significant spin polarization can be switched on and off at the graphene/EuO interface by the gate voltage of the SET: the spin polarization increases from zero to 0.8-1.2, when the gate voltage changes from zero to 0.3 V. The gate voltage dependence of the spin polarization can be explained as follows: At low values of V_g the Fermi energy E_F is below the energy levels $\varepsilon_{d\uparrow}^{(1)}$ and $\varepsilon_{d\downarrow}^{(1)}+U$ (see Eq.(6)), they both are unoccupied, $\langle n_\uparrow\rangle \approx \langle n_\downarrow\rangle \approx 0$, and consequently the last term in the effective magnetic field (15), which is responsible for the MP formation, vanishes and the MP formation is not possible. On the

other hand, when E_F exceeds $\varepsilon_{d\uparrow}^{(1)}$ with increasing V_g, but remains smaller than $\varepsilon_{d\downarrow}^{(1)}+U$, then $\langle n_\uparrow \rangle \approx 1$ and $\langle n_\downarrow \rangle \approx 0$, and B_{eff} in (15) increases and the MP formation starts.

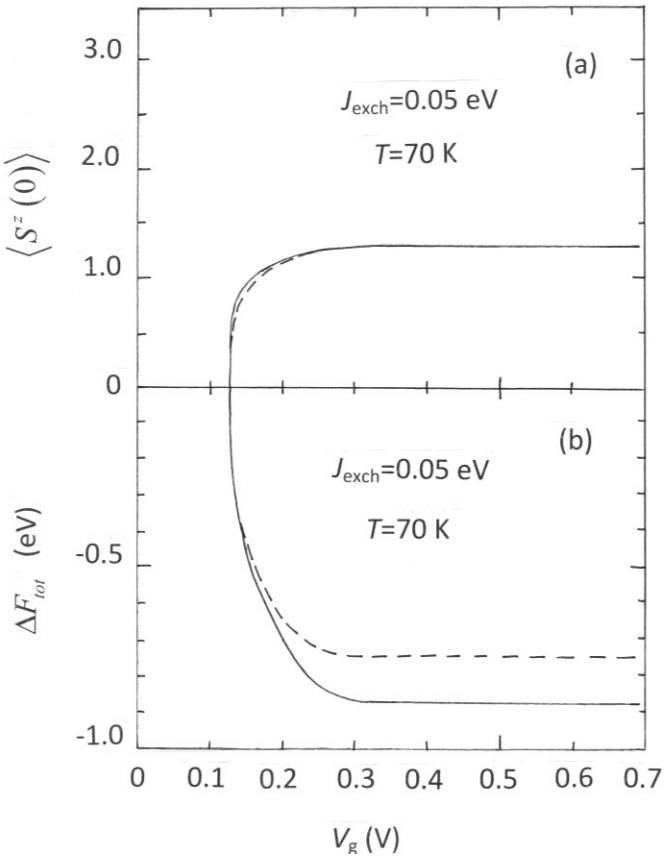

Fig.3. (a) Spin polarization at the graphene/EuO interface at the centre of the QD and (b) the MP binding energy vs. gate voltage at $T=T_C$=70 K in the case of the intermediate coupling J_{exch}=0.05 eV. The solid (dashed) curves have been calculated in the case of the Coulomb repulsion parameter U=0.1 eV (0.02 eV).

Figs. 3 and 4 indicate that a large Coulomb repulsion between the electrons inside the QD favors the MP formation, especially in the case of the weak coupling, J_{exch}=0.02 eV: Fig. 4 shows that the MP binding energy $|\Delta F_{tot}|$ becomes larger when U increases from 0.02 eV to 0.1 eV. This is due to the increase of the effective magnetic field (15) with increasing U, when the energy level $\varepsilon_{d\downarrow}^{(1)}+U$ exceeds E_F, and $\langle n_\downarrow \rangle$ decreases. This is an important advantage in the graphene-based SETs as compared to ordinary semiconductor SETs, since in graphene the permittivity is small [40] and consequently the Coulomb repulsion is large.

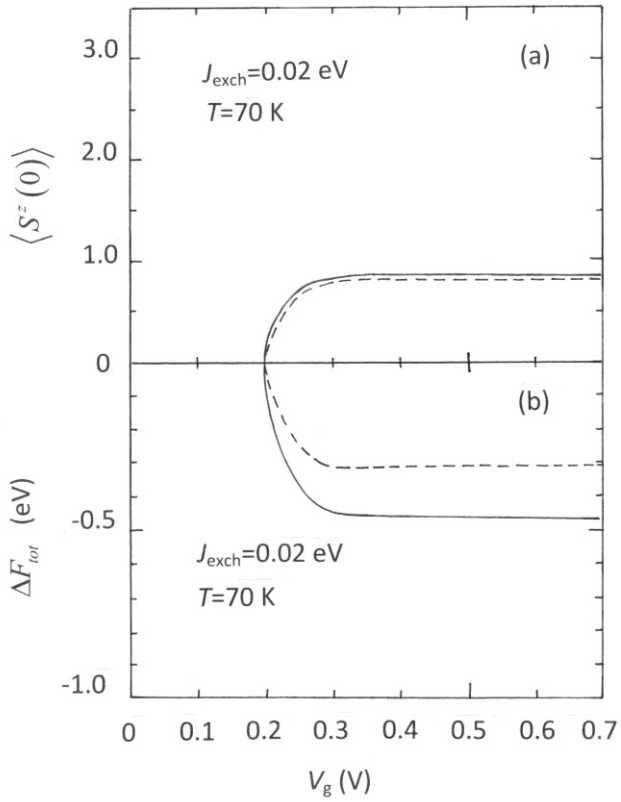

Fig.4. (a) Spin polarization at the graphene/EuO interface at the centre of the QD and (b) the MP binding energy vs. gate voltage at $T=T_C=70$ K in the case of the weak coupling $J_{exch}=0.02$ eV. The solid (dashed) curves have been calculated in the case of the Coulomb repulsion parameter $U=0.1$ eV (0.02 eV).

4 Conclusions We have presented a model for the magnetic polaron formation in ferromagnetic graphene SET. The model predicts that the MP formation enhances the ferromagnetic properties of the graphene/EuO interface in the area of the quantum dot of the SET even in the case of a weak exchange coupling between graphene and EuO. The large Coulomb repulsion between the electrons inside the QD further increases the MP binding energy. We have shown that the spin polarization and the MP binding energy can be controlled by the gate voltage. This could pave the way to novel miniaturized low power memory devices, where the information is stored in the net spin polarization of the QD, and the information content then is read via the current through the graphene SET.

References

[1] K. S. Novoselov, A. K. Geim, S. V. Morozov, D. Jiang, Y. Zang, S. V. Dubonos, I. V. Grigorieva, and A. A. Firsov, Science **306**, 666 (2004).

[2] K. S. Novoselov, A. K. Geim, S.V. Morozov, D. Jiang, M. I. Katsnelson, I. V. Grigorieva, S. V. Duborius, and A. A. Firsov, Nature (London) **438**, 197 (2005).

[3] A. K. Geim and K. S. Novoselov, Nat. Mater. **6**, 183 (2007).

[4] M. C. Lemme, T. J. Echtermeyer, M. Baus, and H. Kurz, IEEE Electron Device Lett. **28**, 282 (2007).

[5] F. Schwierz, Nat. Nanotechnol. **5**, 487 (2010).

[6] O. V. Yazyev, Rep. Prog. Phys. **73**, 056501 (2010).

[7] B. Trauzettel, D. V. Bulaev, D. Loss, and G. Burkard, Nature Phys. **3**, 192 (2007).

[8] P. Recher and B. Trauzettel, Nanotechnology **21**, 302001 (2010).

[9] L. A. Ponomarenko, F. Schedin, M. I. Katsnelson, R. Yang, E. W. Hill, K. S. Novoselov, and A. K. Geim, Science **320**, 356 (2008)

[10] J. Guttinger, T. Frey, C. Stampfer, T. Ihn, and K. Ensslin, Phys. Rev. Lett. **105**, 116801 (2010).

[11] S. Moriyama, Y. Morita, E. Watanabe, D. Tsuya, S. Uji, M. Shimizu, and K. Tshibashi, Sci. Technol. Adv. Mater. **11**, 054601 (2010).

[12] Y. –W. Son, M. L. Cohen, and S. G. Louie, Nature (London) **444**, 347 (2006).

[13] M. Wimmer, I. Adagideli, S. Berber, D. Tomanek, and K. Richter, Phys. Rev. Lett. **100**, 177207 (2008).

[14] W. Y. Kim and K. S. Kim, Nat. Nanotechnology **3**, 408 (2008).

[15] F. Munos-Rojas, J. Fernandez-Rossier, and J. J. Palacios. Phys. Rev. Lett. **102**, 136810 (2009).

[16] W. Han, K. Pi, K. M. McCreary, Y. Li, J. J. I. Wang, A. G. Swartz, and R. K. Kawakami, Phys. Rev. Lett. **105**, 167202 (2010).

[17] B. Dlubak, M.-B. Martin, C. Deranlot, B. Servet, S. Xavier, R. Mattana, M. Sprinkle, C. Berger, W. A. De Heer, F. Petroff, A. Anane, P. Senor, and A. Fert, Nature Physics **8**, 557 (2012).

[18] H.-X. Yang, M.Chshiev, D. W. Boukhvalov, X. Waintal, and S. Roche, Phys. Rev. B **84**, 214404 (2011).

[19] Y. G. Semenov, K. W. Kim, and J. M. Zavada, Appl. Phys. Lett. **91**, 153105 (2007).

[20] H. Haugen, D. Huertas-Hernando, and A. Brataas, Phys. Rev. B **77**, 115406 (2008).

[21] T. Yokoyama, Phys. Rev. B **77**, 073413 (2008).

[22] V. Dam Do, V. Hung Nguyen, P. Dollfus, and A. Bournel, J. Appl. Phys. **104**, 063708 (2008).

[23] J. Zou, G. Jin, and Y. –Q. Ma, J. Phys.: Condens. Matter **21**, 126001 (2009).

[24] V. Hung Nguyen, V. Nam Do, A. Bournel, V. Lien Nguyen and P. Dollfus, J. Appl. Phys. **106**, 053710 (2009).

[25] Y. G. Semenov, J. M. Zavada, and K. W. Kim, Phys. Rev. B **77**, 235415 (2008).

[26] V. Hung Nguyen, A. Bournel, and P. Dollfus, Appl. Phys. Lett. **95**, 232115 (2009).

[27] V. Hung Nguyen, A. Bournel, and P. Dollfus, J. Appl. Phys. **109**, 073717 (2011).

[28] G. M. Roesler, M. E. Filipkowski, P. R. Broussard, Y. U. Idzerda, M. S. Osofsky, and R. J. Soulen, in *Superconducting Superlattices and Multilayers*, edited by I. Bozovic (1994), vol. 2157 of Proc. SPIE, pp. 285-290.

[29] H.-X. Yang, A. Hallal, D. Terrade, X. Waintal, S. Roche, and M. Chshiev, Phys.Rev. Lett. **110**, 046603 (2013).

[30] A. G. Swartz, P. M. Odenthal, Y. Hao, R. S. Ruoff, and R. K. Kawakami, ACS Nano **6**, 10063 (2012).

[31] D. F. Förster, T. O. Wehling, S. Schumacher, A. Rosch, and T. Michely, New Journal of Physics **14**, 023022 (2012).

[32] S. Y. Zhou, G.-H. Gweon, A. V. Fedorov, P. N. First, W. A. De Haar, D.-H. Lee, F. Guinea, A. H. CastroNeto, and A. Lanzara, Nature Materials **6**, 770 (2007).

[33] E. Rotenberg, A. Bostwick, T. Ohta, J. L. McChesney, T. Seyller, and K. Horn, Nature Materials **7,** 258 (2008).

[34] C.-H. Park, F. Giustino, C. D. Spataru, M. L. Cohen, and S. G. Louie, Nano Lett. **9**, 4234 (2009).

[35] G.-Z. Kang, D.-S. Zhang, and J. Li, Phys. Rev. B **88**, 045113 (2013).

[36] G. Giovannenetti, P. A. Khomyakov, G. Brocks, P.J. Kelly, and J. van den Brink, Phys. Rev. B **76**, 073103 (2007).

[37] J. Bai, X. Zhong, S. Jiang, Y. Huang, and X. Duan, Nature Nanotechnology **5**, 190 (2010).

[38] N. Kharche and S. K. Nayak, Nano Lett. **11**, 5274 (2011).

[39] M. Kim, N. S. Safron, E. Han, M. S. Arnold, and P. Gopalan, Nano Lett. **10**, 1125 (2010).

[40] R.M. Abolfath, P. Hawrylak, and I. Zutic, Phys. Rev. Lett. **98**, 207203 (2007).

[41] A.O. Govorov, Phys. Rev. B **72**, 075358 (2005); Phys. Rev. B **72**, 075359 (2005).

[42] A.K. Bhattacharjee and C. Benoit a' la Guillaume, Phys. Rev. B **55**, 10613 (1997); J. Phys. Condens. Matter **9**, 4289 (1997).

[43] A.G. Petukhov and M. Foygel, Phys. Rev. B **62**, 520 (2000).

[44] R. Charrour, M. Bouhassoune, M. Fliyou, D. Bria, and A. Nougaoui, J. Appl. Phys. **88**, 3514 (2000).

[45] A.L. Efros, M. Rosen, and E.I. Rashba, Phys. Rev. Lett. **87**, 206601 (2001).

[46] F. Qu and P. Hawrylak, Phys. Rev. Lett. **96**, 157201 (2006).

[47] H. Enaya, Y.G. Semenov, K.W. Kim, and J.M. Zarada, IEEE Trans. Nanotech. **7**, 480 (2008).

[48] S. Mackowski, T. Gurung, A. Nguyen, H.E. Jackson, and L.M. Smith, Appl. Phys. Lett. **84**, 3337 (2004).

[49] C. Gould, A. Slobodskyy, D. Supp, T. Slobodskyy, P. Grabs, P. Hawrylak, F. Qu, G. Schmidt, and L.W. Molenkamp, Phys. Rev. Lett. **97**, 017202 (2006).

[50] D.M. Hoffman, B.K. Meyer, A.I. Ekimov, I.A. Merkulov, Al.L. Efros, M.Rosen, G. Couino, T. Gacoin, and J.P. Boilot, Solid State Commun. **114**, 547 (2000).

[51] A.A. Maksimov, G. Bacher, A. McDonald, V.D. Kulakovskii, A. Forchel, C.R. Becker, G. Landwehr, and L.W. Molenkamp, Phys. Rev. B **62**, R7767 (2000).

[52] P. Wojnar, J. Suffczynski, K. Kowalik, A. Golnik, G. Karczewski, and J. Kossut, Phys. Rev. B **75**, 155301 (2007).

[53] I. R. Sellers, R. Oszwaldowski, V. R. Whiteside, M. Eginligil, A. Petrou, I. Zutic, W.-C. Chou, W. C. Fan, A. G. Petukhov, S. J. Kim, A. N. Cartwright, and B. D. McCombe, Phys. Rev. B **82**, 195320 (2010).

[54] N. Lebedeva, A. Varpula, S. Novikov, and P. Kuivalainen, Phys. Rev. B **81**, 235307 (2010).

[55] N. Lebedeva, A. Varpula, S. Novikov, and P. Kuivalainen, Phys.Sat. Sol. B **249**, 2244 (2012).

[56] P. W. Anderson, Phys. Rev. **124**, 41 (1961).

[57] H. Bruus and K. Flensberg, Many-Body Quantum Theory in Condensed Matter Physics – An Introduction (Oxford University Press, Oxford 2005).

[58] Jacak, P. Hawrylak, and A. Wojs, Quantum Dots (Springer, Berlin, 1998).

[59] C. Lacroix, J.Phys.F: Metal Phys. **11**, 2389 (1981).

[60] H. Haug and A-P. Jauho, Quantum Kinetics in transport and Optics of Semicondcutors (Springer-Verlag, Berlin, 1998).

[61] J. Kubler, Z.Physik **250**, 324 (1972).

[62] K. Bolotin, F. Ghahari, M. Shulman, H. Stormer, and P. Kim, Nature **462**, 196 (2009).

[63] P. G. Steeneken, L. H. Tjeng, I. Elfimov, G. A. Sawatzky, G. Ghiringhelli, N. B. Brookes, and D. J. Huang, Phys. Rev. Lett. **88**, 047201 (2002).